Analytical model for masonry walls strengthened with vegetal fabric reinforced cementitious matrix (FRCM) composites and subjected to cyclic loads

Luis Mercedes[(2)], Ernest Bernat-Maso[(1)(3)], Lluis Gil[(1)]

[(1)] Department Strength of Materials, Polytechnic University of Catalonia, Terrassa, Spain

[(2)] LITEM Laboratory for Technological Innovation of Structures and Materials, Spain

[(3)] Serra Húnter Fellow

E-mail address: luis.enrique.mercedes@upc.edu; ernest.bernat@upc.edu; lluis.gil@upc.edu.

Abstract

Masonry is one of the eldest construction systems in the building industry, currently in use because some advantages like compressive capacity, traditional aesthetics, low cost and good practices. However, damages recorded in walls as a result of cyclic loads, have given rise to an important development in the area of strengthening and rehabilitation of this type of structural element. To counteract this problem, the vegetal FRCM arises as a strengthening competitive system for the improvement of the mechanical properties of masonry walls. In this study, an analytical model evaluates the behaviour of walls strengthened with FRCM. The model is compared with existing codes and it is validated with experimental results of shear diagonal-compression tests and shear under cyclic loads. It proved to be an effective calculation tool, useful enough to reproduce the behaviour of masonry walls strengthened with FRCM, but limited to failures not related with debonding neither sliding of FCRM material and substrate.

Keywords: Masonry walls, FRCM, Vegetable fibres, Analytical model, Cyclic loading

1. Introduction

The growing concern for the preservation of old buildings and the wide use of masonry in the civil construction works has led to a great innovation in the development of specific techniques to study structures made with these materials.

The mechanical behaviour of masonry structures is more complex than concrete, largely because the masonry consists of two different components, these are the masonry units and the mortar joints. As result, masonry structures are not homogeneous and contain many discontinuities. The degree of complexity is further increased by the inherent variations in materials and variations in the workforce. Therefore, reproducing the real behaviour of this type of structure through an analytical or numerical model is a complex task.

Reliable and accurate analytical methods reveal to be fundamental for engineering calculations and these support the definition of rational design rules.

There are several studies that have already obtained analytical models capable of reproducing the behaviour of masonry walls. One of the most used procedures was presented in [1]. This one identifies 4 types of shear failures in masonry walls, which are validated by the experimental results. The shear failures identified in masonry walls tested at diagonal compression are defined as shear sliding, shear friction, diagonal tension, and toe crushing failures.

A study presented by Silva et al. [2] used the probabilistic Monte Carlo simulation model (MCS) for the evaluation of the shear strength in the reinforced and unreinforced concrete and clay masonry walls. This model was modified and calibrated based on experimental

results. Finally, the proposed analytical model was able to accurately predict failure modes and in-plane shear strength within a 95% confidence interval.

On the other hand, seismic damage has led to an important development of strengthening techniques for masonry structures. In this context, Fabric Reinforced Cementitious Matrix (FRMC) arises as an alternative strengthening system for the improvement of the mechanical properties of masonry structures against seismic actions. Fabric Reinforced Cementitious Matrix (FRCM) is a composite material formed by a mesh embedded in an inorganic mortar matrix, which emerged as a substitute option to the organic matrix of the FRP (Fibre Reinforced Polimers). Since having less toxic emissions, greater fire resistance, water vapor permeability, compatibility with inorganic substrates and removability capacity (except for the case of confinement as stated in [3]), researchers have pointed it as a possible alternative to FRP in the structural strengthening and rehabilitation field.

Numerous researches oriented to experimentally characterize this type of material [4][5][6][7] have been carried out in the recent years. Hence, the development of calculation tools capable of reproducing these experimental studies on masonry walls strengthened with FRCM is a need. In particular, development of analytical models for accurately reproduce the shear behaviour of these structures has been restricted by the difficulties associated to modeling the bond behaviour between FRCM and masonry walls.

Another study published by Cascardi et al. [8] proposed an analytical model to predict the shear strength of masonry strengthened with FRCM using the artificial neural network (ANN) approach, which is inspired by the architecture of the human nervous system consisting of a large number of neurons that are responsible for learning and decision making. In this, a matrix of numerical value weighting and a bias for each neuron is proposed to adjust the model. For the calibration of the model, experimental campaigns of diagonal compression tests carried out on walls strengthened with FRCM were selected and analyzed. The selected database includes a sufficient variety of types of masonry (material and texture), as well as the type of reinforcement, referring to several fibress (glass, carbon, steel, basalt, PBO, etc.) and matrixes (cement, lime, hydraulic mortar). The database developed and the subsequent analysis allowed to provide an effective model to predict the in plane shear strength of masonry walls strengthened with FRCM systems. However, this model not considered masonry strengthened with FRCM of vegetal fibres.

Babaeidarabad et al. [1] uses the methodology proposed by ACI 549 [9] based on the classic formulation of shear strength to analyze the behaviour of strengthened walls with carbon FRCM. This is one of the most used methodology, since it has proven to be effective in predicting the shear strength of masonry walls. Ismail et al. [10] also used this methodology to analyze walls strengthened with glass, basalt and carbon FRCM. In the case of walls strengthened with glass and basalt FRCM, the analytical model showed a conservative shear strength, where the relationship between the predicted and experimental values was 0.38 to 0.71. However, in the case of walls strengthened with carbon FRCM, the shear strength was conservative only when the crush limitation was not verified.

On the other hand, FRCM composites present two technical drawbacks still to be overcome: the high stiffness of synthetic fibre meshes commonly used make the dissipation of energy against cyclic loading difficult, which results in a stress concentration on the existing structure, and secondly, obtaining these used synthetic fibres supposes a high economic and environmental cost.

In view of the above, the use of natural resources and sustainable materials is a topic that is becoming more and more interesting for the scientific community, the alternative of using vegetable fibres as reinforcements of polymers and mortars is an example of this [11][12][13][14][15]. The mechanical properties that fibres such as flax, hemp, sisal, jute or banana among many others have shown, together with their low cost, low density, recyclability and biodegradability, have made vegetable fibres a powerful alternative to synthetic fibres [16].

Despite all these advantages, unfortunately, the organic origin of vegetal fibres favours their degradation in the environment of cementitious matrix composites [17] owing to high alkalinity and humidity cycles. In view of this drawback, some authors have studied the feasibility of applying treatments to avoid the degradation of the fibres. The most popular and easy is the coating of fibres with a resin [18] and it is widely used for commercial meshes applied to the strengthen solutions with FCRM composites. It has been proved that this technique slows down the fibre degradation within the cementitious matrix [19], and in other cases, it improves the mechanical properties and the bond of the meshes with the matrix [20][21]. As a paradox, the resin prevents the degradation of the fibre but at the same time rises down the benefits of sustainability and low cost of the solution. Therefore, for vegetal fabrics used in this study the addition of a coating is justified for the protection of the fibre in an aggressive cementitious matrix, for improving the mechanical and mesh-matrix interaction [15] and finally, as a partial replacement of synthetic fibres with long term durability.

In spite of the numerous studies of masonry walls strengthened with FRCM, in the authors' records there are no studies oriented to the analytical analysis of masonry walls strengthened with FRCM of vegetal fibres (more deformable than synthetic fibres) and subject to shear cyclic loads.

This study represents the continuation of an experimental study previously realized [22]. Therefore, the main objective of this is to develop analytical models capable of reproducing the experimental behaviour.

In this study, four types of masonry walls were analyzed, one unreinforced, one strengthened with hemp FRCM, one strengthened with cotton FRCM and another strengthened with glass FRCM. To do this, modifications were proposed to equations already established, since from the theory of the mixture it was possible to introduce the matrix contributions and the fabric deformation capacity (typically limited to 0.004 in established formulations).

In addition, a coefficient obtained from the relationship of the FRCM materials elastic properties (fabric and matrix) was used together with a stiffness degradation coefficient (not considered in the initial formulation) to approximate analytical to the experimental results. These models were useful to reproduce the behaviour of walls with high compatibility between FRCM-masonry, and mesh-mortar interfaces. Furthermore, the present work incorporates additional results from other experimental studies in order to

increase the testing database and to make the proposed analytical model more representative.

2. Materials Properties

2.1.Masonry

The mechanical properties of masonry walls constructed with fired clay bricks are presented in Table 1. These values were obtained from other studies previously carried out [23][24]. In these, compression tests and shear tests were carried out on the masonry (performed according to the UNE-EN 1052-3: 2003 [25]). The data presented in this table is the necessary one to define the properties of masonry in the analytical models presented in this study.

Table 1. Masonry properties

Compression strength (MPa)	Tensile strength (MPa)	Modulus of deformability (MPa)	Shear strength (MPa)	Coefficient of friction (/)
10.8 (23%)	1.61 (23%)	780 (38%)	0.17	0.73

The values of shear strength (0.17 MPa) and coefficient of friction (0.73) were obtained from the linear regression obtained from 8 experimental tests.

2.2.FRCM

Table 2 shows the properties of the cementitious matrix and the vegetable fibres necessary to define the material properties of the analytical models. These data are obtained from experimental tensile tests on FRCM samples presented in [15]. Also the mesh properties are listed in Table 3 (obtained from [22]).

Table 2. Cementitious matrix and vegetal fibres properties [15]

Properties	Mortar	Hemp	Cotton	Glass
Tensile strength (MPa)	4.61	520.76	91.95	676.76
Compression strength (MPa)	39.25	-	-	-
Modulus of elasticity (GPa)	8.92	38.74	0.93	60.95

Table 3. Mesh properties [22]

Mesh	Hemp		Cotton		Glass	
Tuft direction	**Warp**	**Weft**	**Warp**	**Weft**	**Warp**	**Weft**
Equivalent thickness (mm)	0.08	0.06	0.24	0.18	0.04	0.04
Yarns/tuft (-)	12		6		-	
Tensile strength of mesh (KN/m)	40.88	30.66	32.48	24.36	28.32	28.53
Strain (%)	1.30		7.81		1.22	

Weight/area (g/m^2)	520	771	225

3. Experimental camping and results

3.1.Construction of walls and test setup

Walls of 90×100 cm were designed with fired clay bricks are presented in Table 1, of these walls 2 of them were strengthened with hemp FRCM, 2 were strengthened with cotton FRCM, 2 were strengthened with glass FRCM, 2 were strengthened with only mortar and 2 were left unreinforced. The FRCM thickness was 10mm.

After that the walls were subjected to cyclic load test [26] to study the effectiveness of vegetal fibres FRCM at strengthening masonry. The tests consisted of restraining the horizontal displacement of the wall tops and allowing in-plane displacement of the wall bottoms. A distributed compression load was applied to the wall tops and in-plane lateral cyclic displacement was applied to the wall bottoms (see Figure 1).

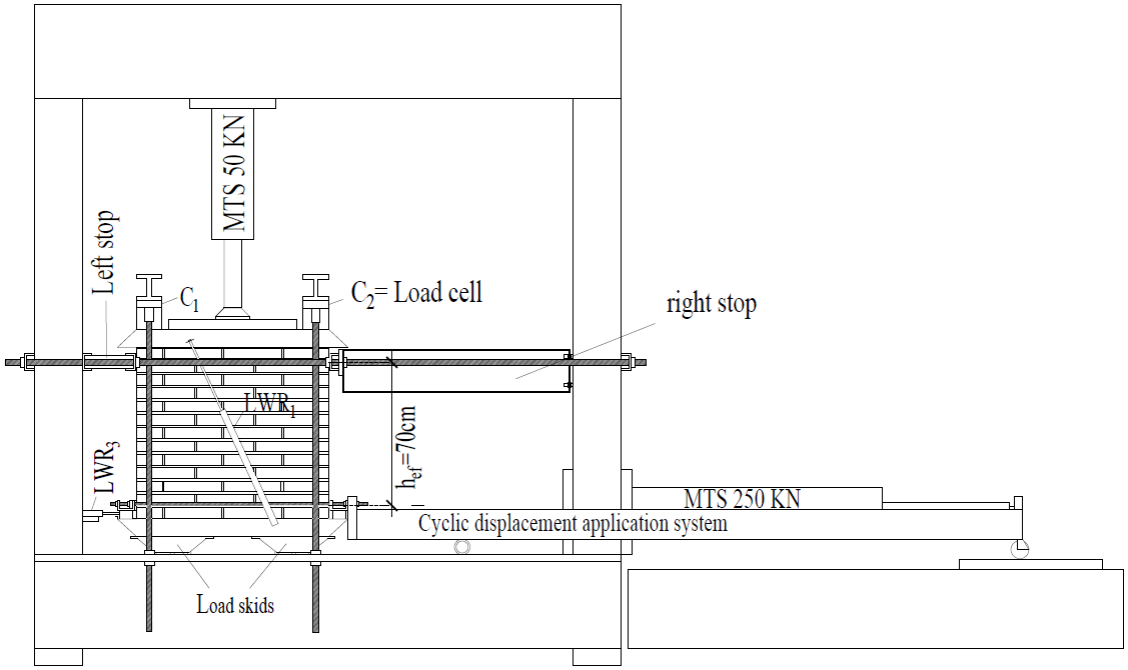

Figure 1. Test setup: in-plane cyclic loading [22]

3.2.Types of failure

The failure of unreinforced walls (WN), walls strengthened with only mortar (WMN), and walls strengthened with glass fibre FRCMs (WG) was characterised by shear crack formation, resulting in two large diagonal cracks (Figure 2).

In the walls strengthened with vegetal fibre FRCMs, cracks were distributed diagonally across the FRCM system and there was detachment of the FRCMs near the corners of the walls, where local masonry failure was observed (see Figure 3). The way in which cracks appeared in these specimens indicates a more favourable distribution of stress in the strengthening systems, as well as the possibility of dissipating additional energy through cracks. However, the fact that the FRCMs detached may indicate that the volume of fibres used affects connection to the matrix [13] until the point of connection failure.

Figure 2. Specimen failures: WN, WNM, and WG

Figure 3. Specimen failures: WH and WC

3.3.Experimental results

A representative diagram of the properties calculated from a hysteresis diagram defined by the envelope and the idealized bilinear model are shown in Figure 4. This bilinear previously used by [27], was used to process the experimental results and to do the analytical approach. This model was chosen because the shear load had fairly sharp drop once reached the maximum shear.

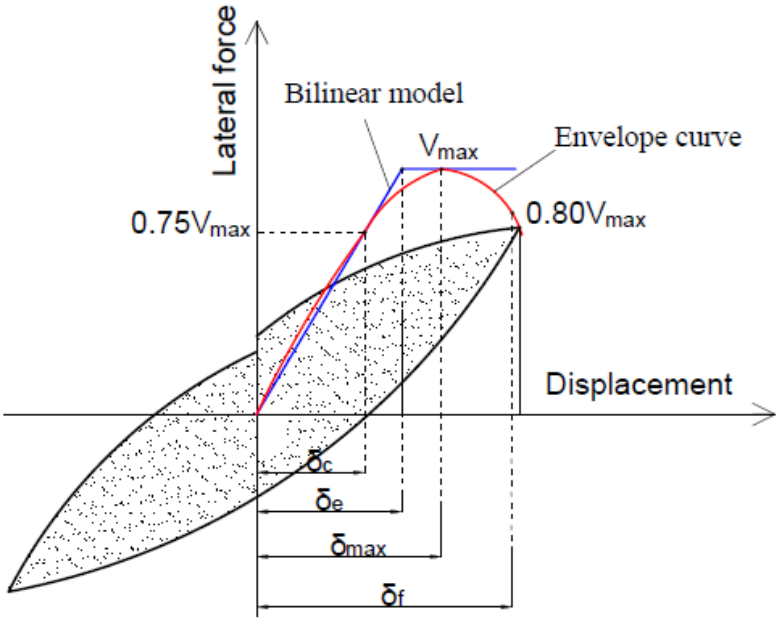

Figure 4. Idealized bilinear model [27]

This model [27] is defined by an equivalent shear to 0.75 of the maximum shear, the maximum shear (V_{max}), the last shear equivalent to $0.80V_{max}$, from which the total failure of the structure, the crack displacement (δ_c), the effective displacement (δ_e) corresponding

to the extrapolation of the limit state of cracking, the displacement where it reaches the maximum shear, and the displacement corresponding to the failure shear (δ_f) can be calculated. The results of the cyclic loading tests are shown in Table 4 (more details are presented in [22]).

Table 4. Results of cyclic loading test

Wall Specimen	V_{max} (KN)	$0.75V_{max}$ (KN)	δ_{max} (mm)	δ_{max}/h (%)	δ_e (mm)	K_e (KN/mm)
Unreinforced	40.54	30.4	7.03	1	4.2	7.25
	(12.39%)	(7.07%)	(13.12%)		(0.82%)	(8.23%)
Only Mortar	105.87	79.4	19.65	2.81	12.39	6.62
	(9.78%)	(5.42%)	(19.47%)		(15.16%)	(6.07%)
Hemp FRCM	156.57	117.43	30.22	4.32	20.53	5.72
	(6.7%)	(3.14%)	(0.18%)		(0.11%)	(3.24%)
Cotton FRCM	162.35	121.76	29.83	4.26	20.86	5.85
	(1.38%)	(0.7%)	(2.68%)		(3.47%)	(2.43%)
Glass FRCM	147.73	110.79	27.13	3.88	19.01	5.85
	(0.19%)	(0.09%)	(12.04%)		(3.48%)	(3.15%)

(CoV %): Coefficient of variation

4. Analytical model

For the analytical study of masonry walls strengthened with FRCM, the method described by ACI 549.4R-13 [9] was used as a reference, where the in-plane nominal shear strength of walls strengthened with FRCM is determined by the following equation:

$$V_n = V_w + V_r \tag{1}$$

Where V_n is the nominal shear strength, V_w is the shear strength of unreinforced walls and V_r is the contribution of shear strength from the FRCM to the wall.

4.1.Unreinforced walls shear strength

To determine the shear strength of the unreinforced walls used in this study, the procedures described in [2][1] were taken as reference. These identify 4 types of shear failures in masonry walls, which were validated by experimental results.

These shear failures are defined as shear sliding, shear friction, diagonal tension, and toe crushing (in the case of walls under diagonal compression testing) failures.

Shear sliding failure occurs due to the failure between the masonry unit and the mortar, resulting in a crack along one horizontal masonry joint. Shear friction failures occur due to joint failure followed by the propagation of the crack through the horizontal and vertical joints. The diagonal tension failure is produced by main tension induced by high compression and shear stresses that exceed the masonry tensile strength. The toe crushing occurs when the stresses generated at the ends of load exceed the compressive strength

of the masonry, this type of failure is presented in the walls tested to diagonal compression, so in this study this type of failure was not considered.

Attending to these types of failures Silva et al. [2] proposed equations to determine the shear strength, taking as a design criterion the use of the minimum value resulting from these 4 equations. Taking into account that this analytical study is carried out for comparative purposes with the experimental results made in this study, the value that best fits the experimental results (failure mode) will be adopted as wall shear strength. Below, the equations for each type of failure are presented:

1. Shear slide failure:

$$V_{ss} = \frac{\tau_0}{1 - \mu_0 tan\theta} An \tag{2}$$

2. Shear friction failure:

$$V_{sf} = \frac{\tau_{0,m}}{1 - \mu_{0,m} tan\theta} An \tag{3}$$

$$\tau_{0,m} = \frac{\tau_0}{1 + 1.5\mu_0(\frac{h}{w})} \tag{4}$$

$$\mu_{0,m} = \frac{\mu_0}{1 + 1.5\mu_0(\frac{h}{w})} \tag{5}$$

3. Diagonal tension failure:

$$V_{dt} = \frac{tan\theta + \sqrt{21.16 + tan^2\theta}}{10.58} f'_{t,w} An \tag{6}$$

Where the one that most closely matches the experimental results (type of failure and shear strength) of V_{ss}, V_{sf} and V_{dt}, will be equal to the shear strength of the unreinforced wall (V_w). τ_0 is the bond strength between mortar and brick joints, μ_0 is the coefficient of shear friction, and θ is the angle between the diagonal of the walls and the horizontal length parallel to the action line of the cyclic load, A_n is the parallel shear are to the direction of the cyclic loads, h y w are the thickness and length of the masonry unit respectively, and $f'_{t,w}$ is the masonry tensile strength calculated from $0.5\sqrt{f'_w}$, being f'_w the masonry compressive strength.

4.2. FRCM contribution to wall shear strength (V_r)

For the determination of the FRCM contribution to in-plane shear strength of strengthened masonry walls, the ACI 549.4R-13 proposes that the tensile strain in the FRCM must be less than or equal to 0.004, and the shear design stress (f_{rv}) for the FRCM is calculated from the following equation:

$$f_{rv} = E_f \varepsilon_{fv} \quad (7)$$

Where E_f is the modulus of elasticity of the fibres.
From the above equation, it is possible to determine the FRCM shear strength contribution with the following equation:

$$V_r = 2nA_f L f_{rv} \quad (8)$$

Where A_f is the area of fibres per unit length, L the length wall parallel to the direction of the shear force applied, and n is the number of meshes used.

4.3.Failure displacement of unreinforced walls

The procedure described in Kwok and Ang [28] was used to calculate the failure displacement (δ_f) as a multiple of the displacement corresponding to the maximum shear (δ_{max}).

$$\delta_f = \alpha \delta_{max} \quad (9)$$

Where α is an experimental constant and the maximum shear can be obtained from:

$$\delta_{max} = \lambda_c \frac{V_{max}}{K_e} \quad (10)$$

Where K_e is the initial stiffness of the wall which is obtained from the modulus of elasticity (E_w) and shear modulus (G_w) of the wall, where:

$$G_w = \frac{E_w}{2(1-v)} \quad (11)$$

$$K_e = \frac{G_w A_n}{h} \quad (12)$$

A_n is the shear area, and h is the effective height of the wall, υ is the Poisson coefficient assumed as 0.2 (suggested by EHE [29]), and λ_c is a factor obtained from a regression analysis performed by Kwok and Ang [28], which results in the following equation:

$$\lambda_c = \frac{1}{\left(0.052 + 0.82 \frac{\sigma_c}{f'_w}\right)} \quad (13)$$

σ_c is the applied compression stress, and f'_w is the compressive strength of the masonry.
Considering that the total failure of the specimens occurred when reaching the maximum shear in the experimental study, for this study it is assumed that $\delta_f = \delta_{max}$.

4.4.Failure displacement of FRCM-strengthened walls

To determine the failure displacement of FRCM reinforced walls, the same equations for unreinforced walls were used with the inclusion of the theory of the mixture:

$$A_h = A_w v_w + A_{FRCM} v_{FRCM} \quad (14)$$

$$E_m = E_w v_w + E_{FRCM} v_{FRCM} \quad (15)$$

Where v_w and v_{FRCM} are the volumetric factors of the masonry wall and the FRCM, A_w and A_{FRCM} are the wall shear area and the homogenized shear area of the FRCM, and E_{FRCM} is the modulus of elasticity of the FRCM which is equal to the modulus of elasticity of the fibres by its volumetric factor, because it defines the elastic behaviour of the FRCM once the matrix reaches the cracking stress.

$$E_{FRCM} = E_f v_f \quad (16)$$

4.5.Results and discussions

4.5.1. Shear strength

Table 5 and Table 6 summarize the analytical results calculated with the model of ACI 549.4R-13 and the results obtained from some adjustments made to this model to improve its approximation and applicability for the prediction of the contribution of the FRCM of vegetable fibres and the contribution of glass FRCM to masonry walls subjected to shear.

Table 5. Results of analysis of shear strength of unreinforced walls

	Properties	Value	Δ (%)
Unreinforced wall	μ_0 (/)	0.73	-
	tanθ (/)	0.78	-
	τ_0 (MPa)	0.17	-
	A_n (mm2)	115200.00	-
	V_{ss} (KN)	45.58	12.43
	V_{sf} (KN)	30.92	-23.73
	V_{sd} (KN)	125.21	208.85

In these tables, the volumetric fraction of fibres (v_f), the volumetric fraction of mortar (v_m), shear strength of the unreinforced wall (V_w), the bond strength between the brick and mortar joint (τ_0) taken from Table 1, the coefficient of shear friction (μ_0) also taken from Table 1, the tangent of the angle between the diagonal of the walls and the horizontal length (tanθ), the shear area (A_n), the stress values (f_{fv}) and shear load (V_f) contributed by the FRCM, calculated from the modulus of elasticity, the maximum displacement and the tensile strength of the fibres and mortar obtained experimentally (see Table 2) are shown. The results presented in Table 5 show that of the calculated shear stresses, the one that most closely approximates the experimental results obtained in this study is the slip failure shear. This also coincides with the failure identified in the specimens of unreinforced

walls tested. Based on this, the shear for slide failure will be considered as the shear strength of the unreinforced wall (V_w).

The results shown in Table 6 show a high difference between the shear strength calculated from model ACI 549.4R-13 and the experimental results obtained in this study, which shows the lack of precision of this model for the considered cases. Hence, it was necessary to modify the original equations in order to adjust analytical results to the experimental results.

Table 6. Results of analysis of shear strength of strengthened walls

	Model	**ACI 549.4R-13**			**Adjusted-ACI 549.4R-13**			**Cascardi**		
Walls strengthened with FRCM	Mesh	Hemp	Cotton	Glass	Hemp	Cotton	Glass	Hemp	Cotton	Glass
	v_f (/)	0.01	0.06	0.01	0.01	0.06	0.01	0.01	0.06	0.01
	v_m (/)	0.99	0.94	0.99	0.99	0.94	0.99	0.99	0.94	0.99
	A_f (mm^2)	144	424	76	144	424	76	144	424	76
	A_m (mm^2)	17856	17492	17352	17856	17492	17352	17856	17492	17352
	$A_{h,FRCM}$ (mm^2)	-	-	-	17633	16529	17224	-	-	-
	$E_f v_f$ (Gpa)	-	-	-	0.49	0.05	0.47	-	-	-
	L (mm)		900			900			900	
	f_{rv} (Mpa)	155	4	245	6.35	4.12	5.75	-	-	-
	φ (/)	-	-	-	1	1.48	1	-	-	-
	V_r (kN)	22.31	1.58	18.52	111.89	68.07	99.1	-	-	-
	V_f (kN)	-	-	-	-	-	-	25.00	12.99	17.05
	V_m(kN)	-	-	-	-	-	-	11.19	11.01	11.23
	V_n (kN)	67.89	47.16	64.1	157.79	168.3	144.8	106.50	87.97	94.40
	Δ (%)	-56.64	-70.95	-56.61	0.78	3.67	-1.97	-31.98	-45.81	-36.10

From the mixture theory of composite materials, and considering the significant strength contribution that showed the walls strengthened with mortar only, the area of the homogenized composite was calculated ($A_{h,\,FRCM}$).

$$A_{h,FRCM} = A_f v_f + A_m v_m \tag{17}$$

Where A_m is the mortar area, and the modulus of elasticity of the FRCM (E_{FRCM}) was determined by the equation (16).

Once the modulus of elasticity of the FRCM is determined, it is possible to determine the shear stress contributed by FRCM, using the fibre peak strain experimentally determined for a tuft (see Table 3), since the experimental results of FRCM showed approximately the same peak strain as the fibre tuft. Therefore, the shear stress contributed by the FRCM will be equal to:

$$f_{rv} = E_{FRCM}\varepsilon_f \tag{18}$$

From this, the shear strength is determined by the equation:

$$V_r = f_{rv} A_{h,FRCM} \tag{19}$$

With the shear strength contributed by the wall and by the determined reinforcement, the nominal strength of the reinforced FRCM wall can be determined by equation (1).

In spite of the previous modifications, the shear strength of walls strengthened with cotton-FRCM was much lower than the experimental results. This can be explained by the low modulus of elasticity and tensile strength that cotton presents compared to the fibres commonly used in FRCM systems such as glass fibres. As a result of this, a coefficient (φ) determined from the relationship between the mechanical properties of the matrix and fibres was determined.

$$\varphi = 1 + \frac{\sigma_m E_m}{\sigma_f E_f} \tag{20}$$

So the nominal shear strength of the walls was determined with the equation:

$$V_n = \varphi (V_w + V_r) \tag{21}$$

The adjusted model was also compared with an analytical approach used in other studies [8] and [30]. Cascardi's model was chosen because it depends from the matrix (V_m is the shear matrix contribution) and fabric properties (V_f is the shear fabric contribution), just like the adjusted model proposed in the present study.

The variations between the adjusted-ACI 549.4R-13, the original ACI 549.4R-13 formulation and the Cascardi's model are presented in Table 6, and can also be seen in Figure 5. In this WH is the walls strengthened with hemp-FRCM, WC with cotton-FRCM and WG with glass-FRCM.

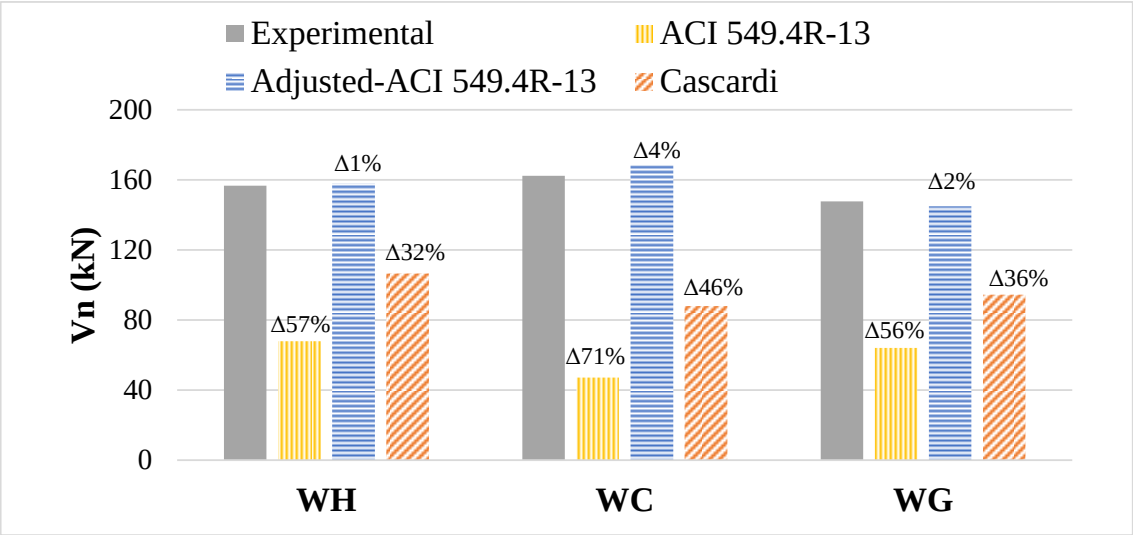

Figure 5. Shear strength: Variation between analytical results and experimental ones

Figure 5 shows how the modifications to the formulations of ACI 549.4R-13 were useful to propose an effective adjusted model to determine the shear strength of walls strengthened with flexible FRCM, which includes glass and vegetal fabrics. The adjusted-ACI 549.4R-13 model presents a better approximation to the experimental results (in contrast to the very conservative results obtained with the ACI 549.4R-13 model), with variations respect to the experimental data from 0.78 to 3.67%. This better approximation is due to the fact that in the adjusted model the contribution of the homogenized area of FRCM is taken into account, and that the strain of the fabric is not limited to 0.4%.

On the other hand, results of the adjusted- ACI 549.4R-13 model also show a better approach than Cascardi's model. This is probably because in the database of the neuronal network approach there were not included any masonry wall strengthened with FRCM of vegetal fibres. Nevertheless, for this problem, the neural network approach performs better than the original ACI549.4R-13 formulation.

4.5.1.1 Comparison with other experimental studies

The analytical approach used in this study is validated reproducing experimental results from other researchers found in the literature. Table 7 shows the materials properties of some FRCM strengthened masonry walls tested with diagonal compression. The analytical nominal shear strength (V_n) calculated with the adjusted model presented in this study is compared to the ultimate experimental load (V_{exp}).

The first thing to highlight in Table 7 is that the value of the coefficient φ is numerically equal to 1 for all cases except for the cotton case as results of computing this variable with equation 20.

Table 7. Comparison of the analytical approach with other experimental results

Specimen	References	Fabric	A_n (mm^2)	f_m (MPa)	A_f (mm^2)	E_f (GPa)	σ_f (MPa)	f_{cm} (MPa)	V_{exp} (kN)	φ (/)	V_n (kN)	Δ (%)	Failures
WH	-	Hemp	115200	10.8	72	38.74	520.76	39.25	156.57	1.00	157.79	0.78	Local failures
WC		Cotton			216	0.93	91.95		162.35	1.48	168.30	3.66	Local failures
WG		Glass			36	60.95	676.76		147.73	1.00	144.83	-1.96	Fabric broke
C-HFC_PT	Menna et al. [11]	Hemp	295000	12.5	284	21.30	169.3	16.10	312.52	1.00	237.16	-24.12	Fabric broke
C-HFC_MW								14.20	318.37	1.00	309.72	-2.71	Fabric broke
NYT-HFC_PT			300000	5.4				16.10	210.89	1.00	240.4	-13.98	Fabric broke
NYT-HFC_MW								14.20	319.09	1.00	325.3	-1.94	Fabric broke
LDB	Garcia-Ramonda et al. [31]	Basalt	393700	17.99		90.00	1700	14.04	295.00	1.00	289.53	-1.85	Fabric broke
LDS		Steel-low density				190.00	2800		279.00	1.00	404.66	45.04	Debonding failures
MDS		Steel-medium density				190.00	3000		227.00	1.00	428.22	88.64	Debonding failures
1 ply	Babaeidarabad et al. [32]	Carbon	105340	24	209	69.00	802	22.00	170.00	1.00	131.16	-22.71	Fabric broke
4 ply					836				329.7	1.00	352.21	6.83	Local failures

f_m= masonry compression strength, σ_f= fabric tensile strength, f_{cm}= FRCM-mortar compression strength, Δ = variation analytical vs experimental results

Notice that the variation between the analytical and experimental loads presented in Table 7 achieves moderate values (between 1-24%) for the failures related with fabric rupture and local damages. On the contrary, for the cases where there is a failure related with debonding or sliding, the variation reaches large values (up to 88%). This limits the use of the analytical approach only for situations where the FRCM has a strong bond with the substrate or when the fabric stiffness is so hight [33].

4.5.2. Failure displacement

The results of the analytical model presented by Kwok and Ang and the corresponding adjusted model are presented in Table 8. Here the modulus of elasticity (E), the shear modulus (G), the shear area (A), are presented. In the case of walls strengthened with FRCM, the value of these properties corresponds to the results of the homogenization using the volumetric factors of the wall (v_w) and the FRCM (v_{FRCM}). The compressive strength (f'_c) and the applied compression stress (σ_c) on masonry are also summarized. For the two models used, the results of initial stiffness (K_e), effective distortion (δ_e/h), distortion at maximum load (δ_{max}/h) and variation of the distortion at maximum load with respect to the experimental results ($\Delta\delta_{max}$) are also presented.

Table 8. Analytical results of fault distortion

Reinforcement		Without	Hemp	Cotton	Glass
Materials properties	v_{FRCM} (/)	-	0.86	0.86	0.86
	v_m (/)	-	0.14	0.14	0.14
	E (MPa)	780	741	648	704
	G (MPa)	325	309	270	293
	A_n (/)	115200	102015	101866	101960
	f'_c (MPa)	10.80	14.41	14.41	14.41
	σ_{cp} (MPa)	0.22	0.25	0.25	0.25
Kwok and Ang model	λ_c (/)	15.04	15.64	15.63	15.64
	K_e (kN/mm)	53.49	44.97	39.27	42.74
	δ_{max}/h (%)	1.78	7.59	9.28	7.34
	$\Delta\delta_{max}/h$ (%)	-77.02	-75.81	-143.94	-112.10
Ajusted-Kwok and Ang model	K (kN/mm)	7.49	6.30	5.50	5.98
	δ_c/h (%)	0.87	3.58	4.37	3.46
	δ_{max}/h (%)	0.97	4.00	4.90	3.87
	$\Delta\delta_{max}$ (%)	3.03	5.96	-14.95	0.08

Table 8 shows a large difference of the failure displacement calculated with the Kwok and Ang model with respect to the experimental results. Because of this, it was necessary to make adjustments to the Kwok and Ang model to have a better approximation to the experimental results obtained.

This adjustment consisted in applying an adjustment coefficient of initial stiffness reduction of 0.14 (obtained of the stiffness relations with the experimental results of all the walls). It was necessary because the initial stiffness calculated was much higher than the initial stiffness experimentally obtained. This coefficient supposes the degradation of

the stiffness by cyclic load until reaching 75% of the maximum shear (see Figure 4). So K_e was calculated with the following equation:

$$K_e = 0.14\frac{GA_n}{h} \tag{22}$$

From this stiffness value, it was possible to determine the value of the effective displacement corresponding to the extrapolation of the cracking limit state(δ_e).

$$\delta_e = \frac{V_{max}}{K_e} \tag{23}$$

Then, from the relation between the failure displacement and the effective displacement experimentally obtained, another experimental coefficient equivalent to 1.12 was determined. Therefore, the fault or maximum displacement is equal to:

$$\delta_{max} = 1.12\delta_e \tag{24}$$

The results presented in Table 8 are better displayed in Figure 6 and Figure 7, where the variations of the analytical results with the experimental results are shown, and the bilinear diagrams resulting from the adjusted analytical models presented in this study are compared to the experimental results.

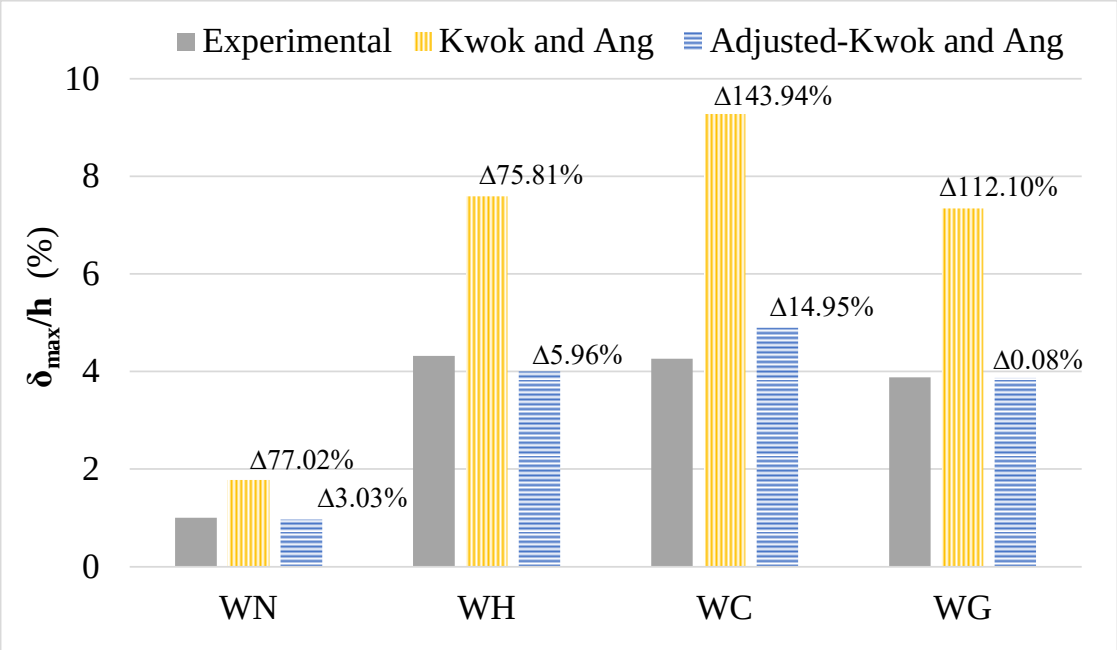

Figure 6. Failure distortion: Variations of analytical results with experimental ones

In Figure 6 it is seen how the Kwok and Ang model presents great variations with respect to the experimental results. This is because the stiffness (K_e) was calculated without taking into account the stiffness degradation due to load cycles.

The results shown in Table 6 and Table 8 indicate a considerable approximation to the experimental results by the adjusted analytical models presented in this study. However, walls strengthened with vegetal fibres presented FRCM detachment failures, which may cause the shear strength and experimental failure displacement not being representative for the case that they reached the tensile fabric break. This analytical model also has the drawback of not being able to reproduce the hysteretic behaviour of the walls, the degradation of stiffness and the amount of energy dissipated by the walls.

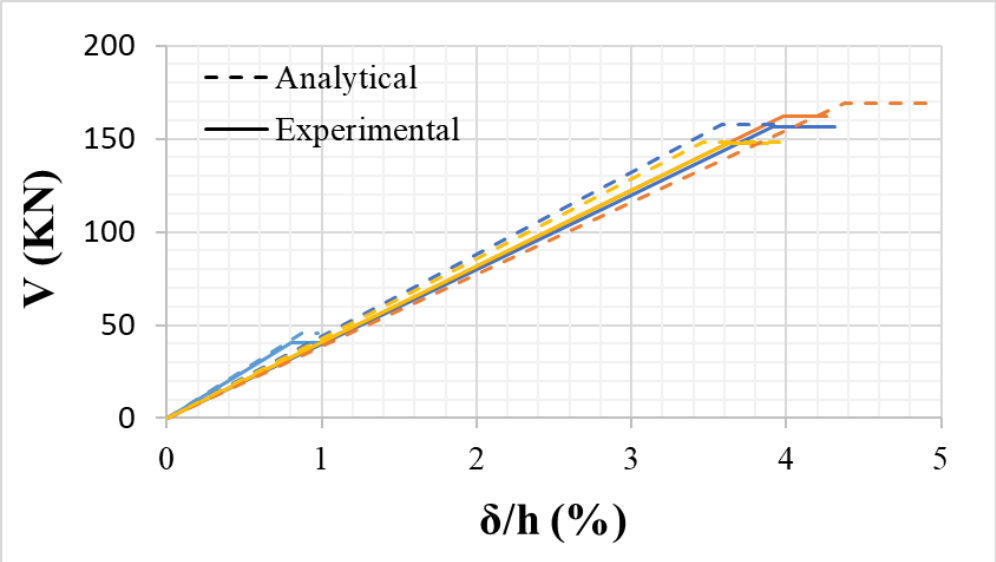

Figure 7. Bilinear curves of analytical model and experimental results: blue = WN, green = WH, orange = WC, yellow = WG

5. Conclusions

From the experimental results of cyclic loading test of walls strengthened with flexible (vegetal or glass fibres) FRCM it was possible to develop analytical models, and compare their results with experimental ones. From the discussion, the following conclusions are reached:

- The ACI 549.4R-13 model was not effective in predicting the shear strength of the walls subjected to cyclic loading because it does not consider the shear strength contribution of the matrix and the shear strength increase due to the deformation capacity of the mesh.
- The Cascardi's model is based in a neural network were no any wall was strengthened with FCRM and vegetal fibres. Therefore, its results differ from the experimental values of the test, but its approach performs better than ACI 549.4R-13 model.
- The Kwok and Ang model was also not effective in predicting the failure distortion of the specimens subjected to cyclic loading. Values of initial stiffness and failure displacements extremely high in contrast with the experimental results.
- To reproduce the experimental results, it was necessary to include a majoring coefficient resulting of the relationship of the elastic properties from FRCM materials (fabric and matrix), and also to include a stiffness degradation coefficient.

- The adjusted models results indicate considerable approximation to the experimental results. Using the mixture law allowed to introduce the matrix contributions and the strain capacity of the fabrics.
- In accordance with the results from other experimental studies, the proposed analytical approach was useful to predict the maximum shear strength when the ultimate load was not reached by debonding neither sliding failure.

Acknowledgements

Authors want to thanks the research project SEVERUS (RTI2018-099589-B-I00) of the Spanish Research Agency. Authors also want to acknowledge the support provided by Bernat Almenar Muns during experimental testing. Second author is a Serra Húnter Fellow.

Conflict of Interest: The authors declare that they have no conflict of interest.

References

[1] S. Babaeidarabad, F. De Caso, D. Ph, A. Nanni, D. Ph, F. Asce, Italian supplier expands its markets, Foundry Trade J. 178 (2004) 242. https://doi.org/10.1061/(ASCE)CC.1943-5614.0000441.

[2] P.F. Silva, P. Yu, A. Nanni, Monte Carlo simulation of shear capacity of URM walls retrofitted by polyurea reinforced GFRP grids, J. Compos. Constr. ASCE. 12 (2008) 405–415. https://doi.org/10.1061/(ASCE)1090-0268(2008)12:4(405).

[3] A. Cascardi, R. Dell'Anna, F. Micelli, F. Lionetto, M.A. Aiello, A. Maffezzoli, Reversible techniques for FRP-confinement of masonry columns, Constr. Build. Mater. 225 (2019) 415–428. https://doi.org/10.1016/j.conbuildmat.2019.07.124.

[4] C. Escrig, L. Gil, E. Bernat-Maso, Experimental comparison of reinforced concrete beams strengthened against bending with different types of cementitious-matrix composite materials, Constr. Build. Mater. 137 (2017) 317–329. https://doi.org/10.1016/j.conbuildmat.2017.01.106.

[5] V. Alecci, F. Focacci, L. Rovero, G. Stipo, M. De Stefano, Intrados strengthening of brick masonry arches with different FRCM composites: Experimental and analytical investigations, Compos. Struct. 176 (2017) 898–909. https://doi.org/10.1016/j.compstruct.2017.06.023.

[6] V. Pino, A. Nanni, D. Arboleda, C. Roberts-Wollmann, T. Cousins, Repair of Damaged Prestressed Concrete Girders with FRP and FRCM Composites, J. Compos. Constr. 21 (2016) 04016111. https://doi.org/http://dx.doi.org/10.1061/(ASCE)CC.1943-5614.0000773.

[7] A. Prota, G. Marcari, G. Fabbrocino, G. Manfredi, C. Aldea, Experimental In-Plane Behavior of Tuff Masonry Strengthened with Cementitious Matrix–Grid Composites, J. Compos. Constr. 10 (2006) 223–233. https://doi.org/10.1061/(ASCE)1090-0268(2006)10:3(223).

[8] A. Cascardi, F. Micelli, M.A. Aiello, Analytical model based on artificial neural network for masonry shear walls strengthened with frm systems, Compos. Part B Eng. 95 (2016) 252–263. https://doi.org/10.1016/j.compositesb.2016.03.066.

[9] ACI committee 549, Gude to design and construction of externally bonded frabric-reinforced cementitious matrix (FRCM) systems for repair and strengthening concrete and masonry structures, 2013.

[10] N. Ismail, T. El-Maaddawy, N. Khattak, A. Najmal, In-Plane Shear Strength Improvement of Hollow Concrete Masonry Panels Using a Fabric-Reinforced

Cementitious Matrix, J. Compos. Constr. 22 (2018) 04018004. https://doi.org/10.1061/(ASCE)CC.1943-5614.0000835.
[11] C. Menna, D. Asprone, M. Durante, A. Zinno, A. Balsamo, A. Prota, Structural behaviour of masonry panels strengthened with an innovative hemp fibre composite grid, Constr. Build. Mater. 100 (2015) 111–121. https://doi.org/10.1016/j.conbuildmat.2015.09.051.
[12] D. Snoeck, P.A. Smetryns, N. De Belie, Improved multiple cracking and autogenous healing in cementitious materials by means of chemically-treated natural fibres, Biosyst. Eng. 139 (2015) 87–99. https://doi.org/10.1016/j.biosystemseng.2015.08.007.
[13] R.S. Olivito, O.A. Cevallos, A. Carrozzini, Development of durable cementitious composites using sisal and flax fabrics for reinforcement of masonry structures, Mater. Des. 57 (2014) 258–268. https://doi.org/10.1016/j.matdes.2013.11.023.
[14] O.A. Cevallos, R.S. Olivito, Effects of fabric parameters on the tensile behaviour of sustainable cementitious composites, Compos. Part B Eng. 69 (2014) 256–266. https://doi.org/10.1016/j.compositesb.2014.10.004.
[15] L. Mercedes, L. Gil, E. Bernat-maso, Mechanical performance of vegetal fabric reinforced cementitious matrix (FRCM) composites, Constr. Build. Mater. 175 (2018) 161–173. https://doi.org/10.1016/j.conbuildmat.2018.04.171.
[16] P. Wambua, J. Ivens, I. Verpoest, Natural fibres: Can they replace glass in fibre reinforced plastics?, Compos. Sci. Technol. 63 (2003) 1259–1264. https://doi.org/10.1016/S0266-3538(03)00096-4.
[17] M. Ardanuy, J. Claramunt, R.D. Toledo Filho, Cellulosic fiber reinforced cement-based composites: A review of recent research, Constr. Build. Mater. 79 (2015) 115–128. https://doi.org/10.1016/j.conbuildmat.2015.01.035.
[18] H. Ahmad, M. Fan, Interfacial properties and structural performance of resin-coated natural fibre rebars within cementitious matrices, Cem. Concr. Compos. 87 (2018) 44–52. https://doi.org/10.1016/j.cemconcomp.2017.12.002.
[19] F. Micelli, M.A. Aiello, Residual tensile strength of dry and impregnated reinforcement fibres after exposure to alkaline environments, Compos. Part B Eng. (2016). https://doi.org/10.1016/j.compositesb.2017.03.005.
[20] J. Donnini, V. Corinaldesi, Mechanical characterization of different FRCM systems for structural reinforcement, Constr. Build. Mater. 145 (2017) 565–575. https://doi.org/10.1016/j.conbuildmat.2017.04.051.
[21] T. D'Antino, C. Papanicolaou, Mechanical characterization of textile reinforced inorganic-matrix composites, Compos. Part B Eng. 127 (2017) 78–91. https://doi.org/10.1016/j.compositesb.2017.02.034.
[22] L. Mercedes, E. Bernat-Maso, L. Gil, In-plane cyclic loading of masonry walls strengthened by vegetal-fabric-reinforced cementitious matrix (FRCM) composites, Eng. Struct. 221 (2020) 111097. https://doi.org/10.1016/j.engstruct.2020.111097.
[23] E. Bernat-Maso, Analysis of unreinforced and TRM-strengthened brick masonry walls subjected to eccentric axial load, Universitat Politècnica de Catalunya, 2013.
[24] E. Bernat-Maso, C. Escrig, C.A. Aranha, L. Gil, Experimental assessment of Textile Reinforced Sprayed Mortar strengthening system for brickwork wallettes, Constr. Build. Mater. 50 (2014) 226–236. https://doi.org/10.1016/j.conbuildmat.2013.09.031.
[25] UNE-EN 1052-3:2003, Methods of test for masonry - Part 3: Determination of initial shear strength, 2003.

588 [26] A. American, N. Standard, Cyclic (Reversed) Load Test for Shear Resistance of
589 Framed Walls for Buildings 1, Assembly. (n.d.) 1–9.
590 [27] N. Ismail, J.M. Ingham, In-plane and out-of-plane testing of unreinforced
591 masonry walls strengthened using polymer textile reinforced mortar, Eng. Struct.
592 118 (2016) 167–177.
593 https://doi.org/http://dx.doi.org/10.1016/j.engstruct.2016.03.041.
594 [28] Y.-H. Kwok, A..-S. Ang, Seismic Damage Analysis and Design of Unreinforced
595 Masonry Buildings, Structural research series no. 536, (1987) 104.
596 https://www.ideals.illinois.edu/handle/2142/14162.
597 [29] EHE-08, Normativa de hormigón estructural en España, 1 (2008) 1689–1699.
598 https://doi.org/10.1017/CBO9781107415324.004.
599 [30] F. Longo, A. Cascardi, P. Lassandro, M.A. Aiello, A new Fabric Reinforced
600 Geopolymer Mortar (FRGM) with mechanical and energy benefits, Fibers. 8
601 (2020). https://doi.org/10.3390/FIB8080049.
602 [31] L. Garcia-Ramonda, L. Pelá, P. Roca, G. Camata, In-plane shear behaviour by
603 diagonal compression testing of brick masonry walls strengthened with basalt
604 and steel textile reinforced mortars, Constr. Build. Mater. 240 (2020) 117905.
605 https://doi.org/10.1016/j.conbuildmat.2019.117905.
606 [32] S. Babaeidarabad, F. De Caso, A. Nanni, URM Walls Strengthened with Fabric-
607 Reinforced Cementitious Matrix Composite Subjected to Diagonal Compression,
608 Asce. 549 (2014) 1–11. https://doi.org/10.1061/(ASCE)CC.
609 [33] O.A. Cevallos, R.S. Olivito, R. Codispoti, L. Ombres, Flax and
610 polyparaphenylene benzobisoxazole cementitious composites for the
611 strengthening of masonry elements subjected to eccentric loading, Compos. Part
612 B Eng. 71 (2015) 82–95. https://doi.org/10.1016/j.compositesb.2014.10.055.
613